



Detection of small single-cycle signals by stochastic resonance using a bistable superconducting quantum interference device

Guozhu Sun, Jiquan Zhai, Xueda Wen, Yang Yu, Lin Kang, Weiwei Xu, Jian Chen, Peiheng Wu, and Siyuan Han

Citation: [Applied Physics Letters](#) **106**, 172602 (2015); doi: 10.1063/1.4919539

View online: <http://dx.doi.org/10.1063/1.4919539>

View Table of Contents: <http://scitation.aip.org/content/aip/journal/apl/106/17?ver=pdfcov>

Published by the [AIP Publishing](#)

Articles you may be interested in

Note: Low temperature superconductor superconducting quantum interference device system with wide pickup coil for detecting small metallic particles

Rev. Sci. Instrum. **83**, 076108 (2012); 10.1063/1.4739311

Characterization of tumors using high- T_c superconducting quantum interference device-detected nuclear magnetic resonance and imaging

Appl. Phys. Lett. **97**, 263701 (2010); 10.1063/1.3530124

Magneto-optical detection of single flux quantum signals in superconducting quantum interference device

Appl. Phys. Lett. **95**, 192503 (2009); 10.1063/1.3262957

Performance of nano superconducting quantum interference devices for small spin cluster detection

J. Appl. Phys. **106**, 023925 (2009); 10.1063/1.3183959

Switching device for the superconducting phase transition measurements of thin W films using a single superconducting quantum interference device

Rev. Sci. Instrum. **70**, 2815 (1999); 10.1063/1.1149800

The advertisement features the Lake Shore Cryotronics logo on the left, which consists of a blue square with a white geometric pattern and the text 'Lake Shore CRYOTRONICS'. In the center is a photograph of the NEW 8600 Series VSM (Vibrating Sample Magnetometer) system, showing a computer monitor, a control panel, and the main measurement unit. On the right, the text reads 'NEW 8600 Series VSM' in large, bold, orange letters, followed by 'For fast, highly sensitive measurement performance' in white. At the bottom right, there is a 'LEARN MORE' button with a right-pointing arrow.

Detection of small single-cycle signals by stochastic resonance using a bistable superconducting quantum interference device

Guozhu Sun,^{1,2,a)} Jiquan Zhai,^{1,2} Xueda Wen,³ Yang Yu,^{4,2} Lin Kang,^{1,2} Weiwei Xu,^{1,2} Jian Chen,¹ Peiheng Wu,^{1,2} and Siyuan Han⁵

¹National Laboratory of Solid State Microstructures and Research Institute of Superconductor Electronics, School of Electronic Science and Engineering, Nanjing University, Nanjing 210093, China

²Synergetic Innovation Center of Quantum Information and Quantum Physics, University of Science and Technology of China, Hefei, Anhui 230026, China

³Department of Physics, University of Illinois at Urbana-Champaign, Urbana, Illinois 61801, USA

⁴School of Physics, Nanjing University, Nanjing 210093, China

⁵Department of Physics and Astronomy, University of Kansas, Lawrence, Kansas 66045, USA

(Received 3 February 2015; accepted 20 April 2015; published online 29 April 2015)

We propose and experimentally demonstrate detecting small single-cycle and few-cycle signals by using the symmetric double-well potential of a radio frequency superconducting quantum interference device (rf-SQUID). We show that the response of this bistable system to single- and few-cycle signals has a non-monotonic dependence on the noise strength. The response, measured by the probability of transition from initial potential well to the opposite one, becomes maximum when the noise-induced transition rate between the two stable states of the rf-SQUID is comparable to the signal frequency. Comparison to numerical simulations shows that the phenomenon is a manifestation of stochastic resonance. © 2015 Author(s). All article content, except where otherwise noted, is licensed under a Creative Commons Attribution 3.0 Unported License.

[<http://dx.doi.org/10.1063/1.4919539>]

It is a long-held belief that noise is detrimental or even destructive to detecting signals which often appear as weak periodic modulations. However, during the last 35 years, theoretical and experimental investigations have shown that in nonlinear systems a proper amount of noise can actually increase the signal-to-noise ratio (SNR) and thus become beneficial for signal detection. This interesting phenomenon is named as stochastic resonance (SR).^{1–4} For example, suppose that a particle is moving in a periodically perturbed symmetric double-well potential under the influence of a Gaussian-white noise such as thermal fluctuation. Then SNR of the power spectral density of the particle's trajectory displays a broad maximum when the rate of inter-well transitions, which depends on noise strength exponentially, is comparable to the frequency of periodic signal. This is the essence of SR.

Due to its simplicity and ubiquity of the underlying mechanism, SR has attracted much interest from physicists, chemists, biologists, and electronic engineers.^{1–11} It has also been observed in Josephson junction-based systems,^{12–16} which have recently attracted much interest and been applied in many fields such as quantum information.^{17–19} However, SR has been only investigated for periodic signals that last many cycles. Namely, only the steady-state properties of the noisy periodically driven systems have been studied. On the other hand, in a variety of science and engineering disciplines, it is a significant challenge to detect small signals which not only last a few cycles but also are buried in noise. Up to this point, whether SR can also enhance single-cycle signal detection remains an open question.

In this letter, we report on the observation of SR in a radio frequency superconducting quantum interference device's (rf-SQUID's)^{20,21} response to weak single-cycle and few-cycle signals by measuring the inter-well transition probability as a function of the noise strength D and the signal frequency f_s systematically. Our experimental and numerical results show that one can distill small single-cycle and few-cycle signals from noisy environment by using bistable systems configured as binary threshold detectors. The maximum sensitivity is achieved at the value of D that matches well with the position of SR. We also show that the sensitivity of detecting single-cycle signals is similar to that of detecting many-cycle signals.

In our experiment, we use an rf-SQUID, which is a superconducting loop of inductance L interrupted by a Josephson junction of critical current I_c , as our bistable detector. An optical micrograph of the sample is shown in the inset of Fig. 1. The Josephson junction is made of Nb/AlOx/Nb on a silicon substrate. The critical current I_c and the capacitance C of the junction are approximately $0.80 \mu\text{A}$ and 90 fF , respectively. The inductance L of the Nb superconducting loop is approximately 1053 pH . The potential energy of the rf-SQUID is given by

$$U(\Phi) = \frac{(\Phi - \Phi_e)^2}{2L} - E_J \cos\left(\frac{2\pi\Phi}{\Phi_0}\right), \quad (1)$$

where Φ_0 is the flux quantum and $E_J = I_c \Phi_0 / 2\pi$ is the Josephson coupling energy of the junction. The shape of the double well potential can be controlled *in situ* by a flux bias Φ_e applied via a flux bias line coupled inductively to the rf-SQUID. In particular, at $\Phi_e = \Phi_0/2$ the SQUID has a symmetric double-well potential separated by a barrier ΔU_0 as

^{a)}Electronic mail: gzsun@nju.edu.cn



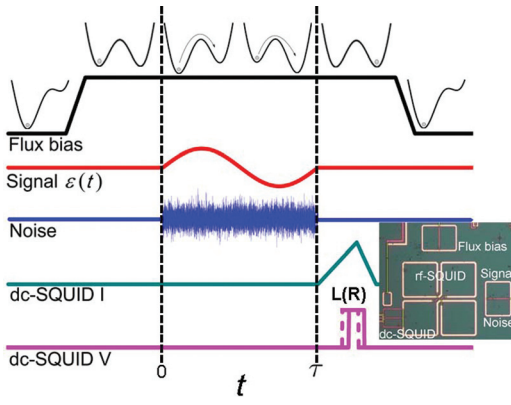


FIG. 1. A time profile of manipulation and measurement. Potential wells at several key moments are also plotted. The inset shows an optical micrograph of a Nb/AlOx/Nb rf-SQUID with an inductively coupled dc-SQUID and flux bias lines.

shown in Fig. 1. For the SQUID studied here, $\Delta U_0/k_B \simeq 12.3$ K, where k_B is the Boltzmann's constant. The dynamics of the rf-SQUID, identical to that of a fictitious flux particle of mass C moving in the potential $U(\Phi)$ with a friction coefficient R^{-1} , is governed by the corresponding Langevin equation

$$C \frac{d^2\Phi}{dt^2} + \frac{1}{R} \frac{d\Phi}{dt} = -\frac{dU}{d\Phi} + I_n(t). \quad (2)$$

Here, I_n is the noise current and R is the damping resistance of the Josephson junction. Without externally injected noise, I_n and R are related by the fluctuation-dissipation theorem $\langle I_n(t)I_n(t') \rangle = \frac{2k_B T}{R} \delta(t-t')$ in thermal equilibrium, where T is temperature. The small oscillation frequency of the system around the bottom of the potential wells is denoted as ω_0 . At $T \gg \hbar\omega_0/k_B$, where \hbar is the Planck constant, thermal activation causes inter-well hopping with the characteristic transition rate given by²²

$$\Gamma_0 = \frac{\omega_0}{2\pi} a_t \exp\left(-\frac{\Delta U_0}{k_B T}\right), \quad (3)$$

where a_t is a damping dependent constant of order of unity. When transitions are dominated by an external noise source of strength $D \gg k_B T$, the denominator in the exponent of Eq. (3) is replaced by D which is proportional to the square of the rms noise current, $I_{n,rms}^2$, applied to the system. For the sake of simplicity, hereafter we set $k_B=1$ so that D is

measured in units of Kelvin. Note that because the potential is symmetric, Γ_0 is identical for left-to-right and right-to-left transitions.

Because all key parameters of the rf-SQUID potential and its control circuit can be accurately determined, the double-well potential of the rf-SQUID is an ideal system for investigating SR^{12–14} and noise-enhanced detection of single-cycle and few-cycle signals. In our experiment, the Gaussian-white noise has a bandwidth of about 9 MHz, which is generated by an arbitrary waveform generator. The signal and noise are applied to the rf-SQUID through a second flux bias line with higher bandwidth (up to 18 GHz). The relationship between D and $I_{n,rms}^2$ is calibrated by measuring Γ_0 versus $I_{n,rms}^2$ and comparing the result to Eq. (3).

As shown schematically in Fig. 1, each measurement cycle begins by ramping up the quasi-static flux bias from 0 to $\Phi_0/2$ to prepare the flux particle in the left side of the symmetric double-well potential. This is followed by applying a single-cycle modulation of flux bias that causes the potential barrier to oscillate as $\Delta U_0 + \varepsilon_0 \sin(2\pi f_s t)$, where ε_0 is proportional to the amplitude of the flux modulation which is kept at $\varepsilon_0 = 0.07\Delta U_0 \simeq 0.86$ K in the experiment. The position of the flux particle is measured by using a dc-SQUID switching magnetometer inductively coupled to the rf-SQUID, either after a single signal cycle or a fixed duration of signal time as discussed later, as a function of $0.5 \text{ K} \leq D \leq 2.0 \text{ K}$ and $10 \text{ kHz} \leq f_s \leq 200 \text{ kHz}$. The quasi-static flux bias is then ramped down to zero to complete the measurement cycle. To obtain the fractional population in the right well ρ_R , the procedure is repeated 2000 times at each value of D and f_s . All data are measured at $T \approx 20 \text{ mK} \ll D$ in a cryogen-free dilution fridge carefully shielded from the environmental electromagnetic interference so that the effects of thermal fluctuation and extra noise on the experiment are negligible.

We first measure ρ_R as a function of the noise strength D by using single-cycle signals $\varepsilon_{\pm}(t) = \pm \varepsilon_0 \sin(2\pi f_s t)$ as depicted in Fig. 1, where the signal frequency $f_s = 10$ kHz. The result is shown in Fig. 2(a). The noise strength D is varied between 0.5 K and 2.0 K. Therefore, transitions between the two potential wells at $\varepsilon_0 = 0$ (no signal) are noise activated. Note that without the noise, $\varepsilon(t)$ alone would be too small to cause transitions between the potential wells because $(\Delta U_0 - \varepsilon_0)/T > 500$. Hence, $D > 0.5$ K is required for the flux particle to hop from one well to the other within

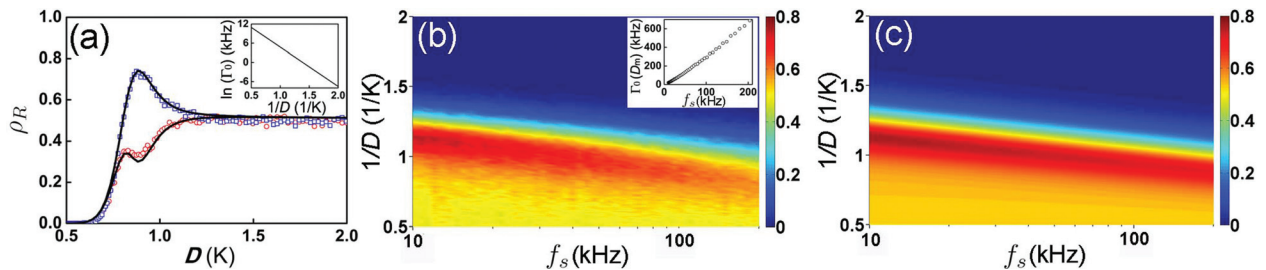


FIG. 2. (a) Measured $\rho_R(D)$ with a single-cycle sinusoidal signal, $f_s = 10$ kHz. Data indicated by the blue squares and red circles correspond to $\varepsilon_+(t)$ and $\varepsilon_-(t)$, respectively, which agree with the numerical calculation (black lines). The inset shows the linear dependence of $\ln(\Gamma_0)$ on $1/D$. (b) ρ_R as a function of $1/D$ and f_s with single-cycle sinusoidal signals $\varepsilon_+(t) = \varepsilon_0 \sin(2\pi f_s t)$. As shown in the inset, when ρ_R reaches a maximum, $\Gamma_0(D_m) \sim 2f_s$, where D_m denotes the noise strength corresponding to maximum ρ_R . These results are consistent with the theoretical hypothesis of SR. (c) Numerical calculation of ρ_R as a function of $1/D$ and f_s with single-cycle sinusoidal signals $\varepsilon_+(t) = \varepsilon_0 \sin(2\pi f_s t)$, which agree well with the experimental data.

the duration of each signal cycle. On the other hand, at $\varepsilon_0 = 0$ the transition rate Γ_0 grows exponentially from approximately 1/s at $D = 0.5$ K to greater than 10^7 /s at $D = 2.0$ K, as shown in the inset of Fig. 2(a). It can be seen that for $D \leq 0.7$ K the population of the right well ρ_R is negligible at $t = \tau = 1/f_s$. The data indicated by the blue squares in Fig. 2(a) are taken with $\varepsilon_+(t)$ which show that as D is increased from 0.7 K, ρ_R rises rapidly to reach maximum when $\Gamma_0(D_m) \sim 2f_s$, where D_m denotes the noise strength corresponding to the maximum ρ_R . When $D > D_m$, the probability of hopping back from the right well to the left well increases rapidly, causing $\rho_R(D)$ to decrease. Finally, when $D \gg \varepsilon_0$ the population of each potential well is equalized to 50%.

SR has two most prominent signatures: One is the peak in the system's response versus noise strength D . The other is the position of the peak and the signal frequency satisfying $\Gamma_0(D_m) \sim 2f_s$, or equivalently, $1/D_m \sim -\ln(f_s)$ according to Eq. (3). In Fig. 2(b), where $\varepsilon_+(t)$ is applied, we plot ρ_R versus $1/D$ and f_s which shows clearly both signatures of SR. In particular, the nearly linear relationship between $\Gamma_0(D_m)$ and f_s is demonstrated as shown in the inset of Fig. 2(b). The slope of $\Gamma_0(D_m)$ versus f_s obtained from the best-fit to a line is 2.7, which is consistent with the numerical result previously obtained for SR under continuous modulation.²³ In addition, we numerically calculate the power spectral density $S(f_s)$ of the flux particle's trajectories $\Phi(t)$ generated by Monte Carlo simulation of Eq. (2). It is found that $S(f_s)$ reaches its maximum at the same value of D as ρ_R does. We thus conclude that SR plays a central role in the bistable system's response to single-cycle signals.

In order to compare the result of our measurements with that of numerical study over the entire parameter space covered by the experiment, we adopt the two-state model^{4,24} and introduce the rate equation

$$\frac{d\rho_R(t)}{dt} = -\Gamma_- \rho_R(t) + \Gamma_+ [1 - \rho_R(t)], \quad (4)$$

with the initial condition $\rho_L(0) = 1$, $\rho_R(0) = 0$. Here, ρ_R ($\rho_L = 1 - \rho_R$) is the fractional population of the right (left) potential well. When $\varepsilon_0 \neq 0$, the barrier height is oscillating between $\Delta U_0 \pm \varepsilon_0$ and the transition rates are time-dependent

$$\Gamma_{\pm}(t) = \Gamma_0 \exp \left[-\frac{\pm \varepsilon_0 \sin(2\pi f t)}{D} \right], \quad (5)$$

where Γ_+ and Γ_- denote the rates of left-to-right and right-to-left transitions, respectively. Γ_0 is given by Eq. (3). Using

the system parameters given above, we numerically integrate Eq. (4) to obtain $\rho_R(t)$ as a function of f_s and D . The result is shown in Fig. 2(c). It can be seen that the key features of the experimental data are well reproduced.

Next, we show that the sensitivity of detecting single-cycle signals is comparable to that of detecting many-cycle signals and that one can predict the population distribution of the bistable systems at the end of N -cycle modulations $\rho_{R,N} \equiv \rho_R(N\tau) = 1 - \rho_{L,N}$ from that of single-cycle modulation $\rho_{R,1}$. It is straightforward to obtain the recursion relation

$$\begin{aligned} \rho_{R,n+1} &= \rho_{L,n} P_+ + \rho_{R,n} (1 - P_-) \\ &= (1 - \rho_{R,n}) P_+ + \rho_{R,n} (1 - P_-). \end{aligned} \quad (6)$$

The first (second) term of the r.h.s. of Eq. (6) is the fractional population of the left (right) well at $t = n\tau$ that ends (remains) in the right well at $t = (n+1)\tau$. $P_{+(-)}$ is the probability of switching from the left (right) to the right (left) well during the time interval $n\tau \leq t \leq (n+1)\tau$. Notice that with the single-cycle perturbation $\varepsilon_{\pm}(0 \leq t \leq \tau)$ and the initial condition $\rho_{R,0} = 0$, one has $P_{\pm} = \rho_{R,1}$ by taking into consideration the spatial and temporal symmetry properties of the rf-SQUID potential and ε_{\pm} . Thus, we can obtain P_{\pm} directly from the data presented in Fig. 2(a). Because Eq. (6) is valid for arbitrary noise strength D and signal frequency f_s , we can compute $\rho_{R,N}$ from P_{\pm} for any integer $N > 1$. We find that as N increases $\rho_{R,N}$ converges rapidly. In order to investigate the dependence of SR on the number of signal cycles N , we modify the experimental procedure by changing the duration of the applied signal and noise from τ to 0.3 ms. Thus, we have $N = 3$ for $f_s = 10$ kHz, which increases ultimately to $N = 60$ for $f_s = 200$ kHz. In Fig. 3(a), the measured $\rho_{R,N}$ is plotted against $1/D$ and f_s , which compares well with $\rho_{R,N}$ computed from Eq. (6) by using the measured P_{\pm} as inputs [see Fig. 3(b)] and that obtained by solving the corresponding rate equation (4) [see Fig. 3(c)]. The results presented in Fig. 3 all have two distinctive features: (i) The threshold noise strength D_0 which demarcates the blue region ($\rho_{R,N} \approx 0$) and the yellow region depends weakly on the number of signal cycles N and (ii) $1/D_m \propto -\ln(f_s)$ remains valid for the entire range of $3 \leq N \leq 60$. As shown in the inset of Fig. 3(a), the dependence of $\Gamma_0(D_m)$ on f_s is approximately linear with a slope of about 2.6. These two features strongly indicate that the sensitivity of detecting single-cycle signals is similar to that of many-cycle and continuous wave signals and that SR does exist in the systems driven by small single-cycle signals.

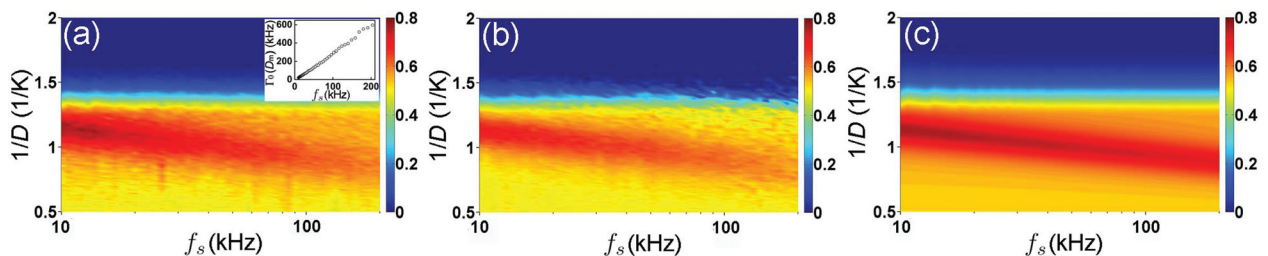


FIG. 3. (a) Measured ρ_R as a function of $1/D$ and f_s with a constant duration (0.3 ms). SR remains as shown in the inset. (b) ρ_R as a function of $1/D$ and f_s with a constant duration (0.3 ms), derived from the recursion relation Eq. (6) and P_{\pm} obtained from the experimental results when single-cycle signals are used. (c) Numerical calculation of ρ_R as a function of $1/D$ and f_s with a constant duration (0.3 ms).

In summary, using an rf-SQUID as a prototypical bistable system, we have demonstrated the existence of SR with single-cycle perturbation to the symmetric double-well potential of the system. Furthermore, we have investigated the possibility of exploiting SR for detecting small single-cycle and few-cycle signals in noisy environment. We have found that a proper amount of noise can lead to SR which enhances the sensitivity of detection. Our work provides insights into the behavior of bistable systems under the combined influence of weak single-cycle (or few-cycle) periodic modulation and noise. Because conventional techniques, such as phase sensitive lock-in and heterodyne detection schemes, are not applicable to detecting single-cycle and few-cycle signals buried in noise, the method demonstrated here is promising for applications where signals are unavoidably mixed up with noise and only last a very small number of cycles.

We thank Dan-Wei Zhang and Shi-Liang Zhu for the valuable discussions. This work was partially supported by MOST (Grant Nos. 2011CB922104 and 2011CBA00200), NSFC (11474154, BK2012013), PAPD, a doctoral program (20120091110030), and Dengfeng Project B of Nanjing University. S.H. was supported in part by NSF (PHY-1314861).

¹K. Wiesenfeld and F. Moss, *Nature* **373**, 33 (1995).

²L. Gammaitoni, P. Hänggi, P. Jung, and F. Marchesoni, *Rev. Mod. Phys.* **70**, 223 (1998).

- ³G. Harmer, B. Davis, and D. Abbott, *IEEE Trans. Instrum. Meas.* **51**, 299 (2002).
- ⁴T. Wellens, V. Shatokhin, and A. Buchleitner, *Rep. Prog. Phys.* **67**, 45 (2004).
- ⁵R. Löfstedt and S. N. Coppersmith, *Phys. Rev. Lett.* **72**, 1947 (1994).
- ⁶M. Grifoni and P. Hänggi, *Phys. Rev. Lett.* **76**, 1611 (1996).
- ⁷S. F. Huelga and M. B. Plenio, *Phys. Rev. Lett.* **98**, 170601 (2007).
- ⁸R. Almog, S. Zaitsev, O. Shtempluck, and E. Buks, *Appl. Phys. Lett.* **90**, 013508 (2007).
- ⁹E. Martinez, G. Finocchio, and M. Carpentieri, *Appl. Phys. Lett.* **98**, 072507 (2011).
- ¹⁰F. Hartmann, L. Gammaitoni, S. Hfing, A. Forchel, and L. Worschech, *Appl. Phys. Lett.* **98**, 242109 (2011).
- ¹¹K. Nishiguchi and A. Fujiwara, *Appl. Phys. Lett.* **101**, 193108 (2012).
- ¹²R. Rouse, S. Han, and J. E. Lukens, *Appl. Phys. Lett.* **66**, 108 (1995).
- ¹³A. D. Hibbs, A. L. Singsaas, E. W. Jacobs, A. R. Bulsara, J. J. Bekkedahl, and F. Moss, *J. Appl. Phys.* **77**, 2582 (1995).
- ¹⁴A. M. Glukhov, O. G. Turutanov, V. I. Shnyrkov, and A. N. Omelyanchouk, *Low Temp. Phys.* **32**, 1123 (2006).
- ¹⁵G. Sun, N. Dong, G. Mao, J. Chen, W. Xu, Z. Ji, L. Kang, P. Wu, Y. Yu, and D. Xing, *Phys. Rev. E* **75**, 021107 (2007).
- ¹⁶C. Pan, X. Tan, Y. Yu, G. Sun, L. Kang, W. Xu, J. Chen, and P. Wu, *Phys. Rev. E* **79**, 030104 (2009).
- ¹⁷J. You and F. Nori, *Phys. Today* **58**(11), 42 (2005).
- ¹⁸J. You and F. Nori, *Nature* **474**, 589 (2011).
- ¹⁹Z.-L. Xiang, S. Ashhab, J. Q. You, and F. Nori, *Rev. Mod. Phys.* **85**, 623 (2013).
- ²⁰R. Rouse, S. Han, and J. E. Lukens, *Phys. Rev. Lett.* **75**, 1614 (1995).
- ²¹G. Sun, X. Wen, Y. Wang, S. Cong, J. Chen, L. Kang, W. Xu, Y. Yu, S. Han, and P. Wu, *Appl. Phys. Lett.* **94**, 102502 (2009).
- ²²P. Hänggi, P. Talkner, and M. Borkovec, *Rev. Mod. Phys.* **62**, 251 (1990).
- ²³R. F. Fox and Y.-N. Lu, *Phys. Rev. E* **48**, 3390 (1993).
- ²⁴B. McNamara and K. Wiesenfeld, *Phys. Rev. A* **39**, 4854 (1989).